Systematic Site-Directed Mutagenesis of Human Protein SRP54: Interactions with Signal Recognition Particle RNA and Modes of Signal Peptide Recognition

Qiaojia Huang,[‡] Sayran Abdulrahman,[§] Jiaming Yin, and Christian Zwieb*

Department of Molecular Biology, The University of Texas Health Science Center at Tyler, P.O. Box 2003, Tyler, Texas 75710

Received March 4, 2002; Revised Manuscript Received July 15, 2002

ABSTRACT: The amino acid residues of human protein SRP54 which are required for binding to SRP RNA were identified by generating 40 nonoverlapping tri-alanine alterations within its methionine-rich M-domain (SRP54M). The mutant polypeptides were expressed in *Escherichia coli*, and their ability to bind to human and *Methanococcus jannaschii* SRP RNA were determined in vitro. Residues at positions 379−387, 394−396, 400−405, and 409−411 of human SRP54 were within the predicted RNA binding site, and their alteration abolished the binding activities of the mutant polypeptides as expected. Changes at positions 418−423 had intermediate effects. Polypeptides containing mutations of 328-TLR-330 were inactive although these residues were far away from the presumed RNA binding site in the crystal structure of the free protein. Using the structures of the *E. coli* Ffh/4.5S core and of the human SRP54m dimer as templates, a molecular model of the complex between human SRP RNA helix 8 and a single SRP54M molecule was constructed in which Leucine 329 was positioned in closer proximity to the RNA binding domain. This representation was supported by studies of the SRP54m monomer/dimer ratio using gel filtration. The results were consistent with a change in the shape of the signal peptide binding groove upon binding of SRP54 to SRP RNA. We propose that the SRP RNA and a small region centered at a bulky nonpolar amino acid residue at position 329 of protein SRP54 play a critical role in the SRP-dependent binding and release of signal peptides.

The cytosolic signal recognition particle (SRP) interacts with the signal peptide of a secretory protein as it emerges from the ribosome. Upon recognition of the signal sequence, SRP pauses translation and allows the ribosome to bind to the SRP receptor on the ER membrane. These events ensure the efficient delivery of proteins to the proper cellular compartment and have been reviewed recently (*1*). SRP-mediated protein targeting is of considerable importance in the cell biology of all organisms, as indicated by the widespread phylogenetic distribution of signal sequences and components of the SRP (*2*, *3*). Every SRP possesses an SRP RNA, named 4.5S RNA in bacteria, and protein SRP54 or Ffh (*4*−*6*). The SRPs of eukarya, archaea, and certain bacteria include additional polypeptides (*2*). For example, mammalian SRP contain the SRP9/14 heterodimer, as well as proteins SRP19, SRP68, and SRP72 (*4*).

Understanding the details of SRP-directed protein targeting requires the identification and molecular characterization of the SRP components. The secondary structures of numerous SRP RNAs were determined by comparative sequence analysis to reveal eight helices, numbered from 1 to 8 (*7*). Helix 8 of the SRP RNA is an essential constituent of the SRP and conserved in sequence and structure. NMR and crystallographic methods were used to resolve the high-resolution structure of *Escherichia coli* 4.5S RNA in the region that corresponds to helix 8 (*8*, *9*). The crystal structure of the 4.5S/Ffh core of *E. coli* SRP provided molecular details of the SRP54 SRP RNA interface and suggested a proximity between the signal peptide and the phosphate-backbone edge of the distal portion of SRP RNA helix 8 (*10*). In the multicomponent SRPs of eukaryotes and archaea, helix 8 was shown to regulate the assembly of the particle by controlling the SRP19-dependent binding of protein SRP54 (*11*−*13*).

SRP54 and its homologues are composed of the N-terminal domain, the centrally located GTPase domain, and the methionine-rich M-domain (SRP54M) (*14*, *15*). SPR54M bound not only to the SRP RNA (*16*), but also was shown by chemical cross-linking to be in close proximity to the signal peptide (*15*, *17*). The crystal structure of the *Thermus aquaticus* Ffh trimer suggested that the signal peptide reached into a short wide pocket formed by the so-called "finger loop" (*18*). Similarly, the structure of the human SRP54m dimer offered the possibility that α-helices 1 and 2 were bound within a long narrow constricted groove generated by the neighboring molecule (*19*). The shape of the groove accommodated the known α-helical character and charge distribution of hydrophobic signal peptides (*20*).

SRP-mediated protein targeting requires a cycle of reactions that involve free SRP, as well as interactions with the ribosome and components of the membrane. Recent evidence derived from the structures of free and RNA-bound protein

* Corresponding author. Address: Department of Molecular Biology, The University of Texas Health Science Center at Tyler, 11937 US Highway 271, Tyler, TX 75708-3154. Tel: (903) 877-7689. Fax: (903) 877-5731. E-mail: zwieb@uthct.edu.

[‡] Current address: Department of Immunology, Box 178, MD Anderson Cancer Center, 7777 Knight Road, Houston, TX 77054

[§] Current address: Internal Medicine Residency, Prince George's Hospital Center, 3001 Hospital Drive, Cheverly, MD 20785.

10.1021/bi025765t CCC: $22.00
Published on Web 08/24/2002

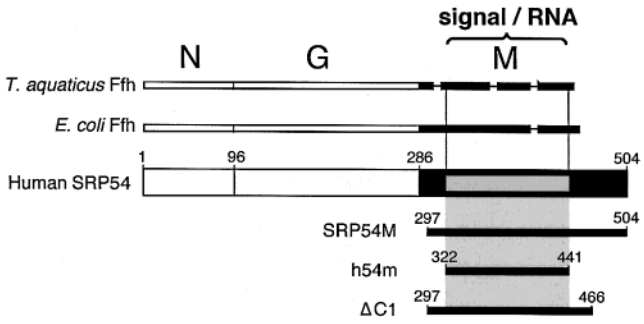

FIGURE 1: Alignment of human protein SRP54 (bottom) and the homologous bacterial polypeptides of *T. aquaticus* (top) and *E. coli* (center). Amino acid residues are numbered according to the human SRP54 sequence. The N-terminal (N) and the GTPase domains (G) are labeled as such. Regions that correspond to the methionine-rich M-domain (M) and polypeptides SRP54M, h54m, and ΔC1 are indicated. The region that was subjected to systematic site-directed mutagenesis is highlighted in gray.

SRP54 and its bacterial homologues (*10*, *18*, *19*) has suggested that the signal peptide groove might undergo dynamic changes under the influence of the signal peptide, protein SRP54, and the SRP RNA. However, the details of these possible sequential dynamic interactions have remained undetermined.

Using systematic site-directed mutagenesis, we have introduced alterations in human SRP54M to identify the amino acid residues required for interaction with SRP RNA. Mutations that abolished or reduced RNA binding were located within a well-defined region that included α-helices 3−7 (*19*). Indicative of an SRP RNA-dependent conformational change in SRP54M, residues that included Leucine 329 were required also. We propose that SRP54 binds and releases the signal peptide by altering the conformation of the signal peptide binding groove mediated by the RNA and a bulky nonpolar amino acid residue at position 329.

RESULTS AND DISCUSSION

Systematic Site-Rirected Mutagenesis of Human SRP54M-ΔC1. Using the PCR-based approach described in Materials and Methods, forty tri-alanine mutant derivatives of SRP54M-ΔC1 (*21*), named A1−A40, were constructed. Amino acid triplets were changed in a nonoverlapping continuous fashion between positions 322 and 441 of human SRP54 covering a region that had been shown to cross-link to the signal peptide of a nascent secretory protein and bound SRP RNA as an independent domain. Polypeptide SRP54M-ΔC1 (170 amino acid residues, 19 105 Da, abbreviated here as ΔC1, Figure 1) was selected as the substrate for the mutagenesis because it migrated in a region of the SDS polyacrylamide gel that was devoid of other proteins, and thus we were able to measure the SRP RNA binding activities without the elaborate purification of each mutant protein. The mutagenic oligonucleotides were designed with a unique *Not*I restriction site to facilitate the identification of the mutant constructs. Alanine substitutions were chosen because of the propensity of Alanine to preserve the α-helical character of SRP54M (*19*, *22*). Mutants A3a, A3b, and A3c were generated subsequently in order to investigate more cosely the role of the Leucine residue at position 329. The locations of the altered amino acids within the sequence of SRP54M are shown in Figure 2.

RNA Binding Activities of the Mutant Polypeptides. Mutant polypeptides were expressed in *E. coli* cells, and lysates were prepared and used directly in binding assays as described in Materials and Methods. Full-length *M. jannaschii* and not human SRP RNA was used as the substrate because the latter required SRP19 to bind SRP54 (*4*, *16*). This simplification of the assay was justified because the SRP RNAs of archaea and eukarya are conserved and functionally interchangeable (*24*). Mutants A7, A19, A23, A26, A29, and A3b were tested also with human SRP RNA. With the exception of the SRP19-dependency of the reaction, there were no differences in their ability to interact with both RNAs (not shown).

Polypeptides ΔC1 and ΔRL (158 amino acid residues, 17 870 Da) were used as controls, the latter construct being identical to ΔC1 but containing a deletion of 12 amino acid residues in the predicted RNA binding region (Figure 2). Proteins were collected from small DEAE columns either in the low-salt flowthrough (F) or the high-salt eluate (E) and analyzed by SDS PAGE as described in Materials and Methods. Results are shown in Figure 3A for mutants A3, A3a, A3b, A7, A20, A30, A33, and A39 and compiled in Table 1. The majority of mutants bound to RNA either completely or not at all. When polypeptides were expressed at exceptionally high levels or an excess of lysate was used, the appearance of active protein in the flowthrough was entirely due to the saturation of available RNA binding sites since complete binding was achieved by decreasing the protein amounts (Figure 3B). Two exceptions were mutants A33 and A34, which displayed binding activities between 33% and 51% for all tested protein concentrations. Most likely, due to variable experimental manipulations, the standard errors of the binding activities of A33 and A34 were unusually high (see Table 1). Interestingly, in parallel experiments, A33 was always more active than mutant A34. It should be mentioned that A19 and A37 contained unanticipated single amino acid substitutions outside the RNA binding and, in fact, the activities of these mutant proteins were preserved (see Table 1). In summary, 30 mutants were fully active, two polypeptides demonstrated intermediate activities, and binding to SRP RNA was abolished in eight of the tri-alanine mutant polypeptides.

The altered residues of the seven mutant polypeptides A20, A21, A22, A25, A27, A28, and A30 that had lost the ability to bind to SRP RNA were clustered near the C-terminus of SRP54M in a region that had been implicated from the crystal structure of h54m to be involved in SRP RNA binding (*19*). Indeed, the homologous area was found to be in contact with 4.5S RNA in the *E. coli* SRP core structure (*10*). Surprisingly, mutant A3 was incapable of binding although the altered residues at positions 328−330 belonged to the N-terminal region of helix 1 which was far away from the RNA binding site (Figure 4A). The flanking mutant polypeptides A2 and A4 bound RNA completely, indicating that a critical change had been introduced into a very short region. To investigate further the role of the three residues at positions 328−330, we constructed mutants A3a and A3b with alterations of only two residues and a common Leucine to Alanine change at position 329. A residual RNA binding activity of about 6% for mutant A3a and the complete inactivity of mutant A3b suggested a crucial role of L329 in RNA binding (see Figure 2 and Table 1). Mutant A3c contained a single L329A change which preserved the

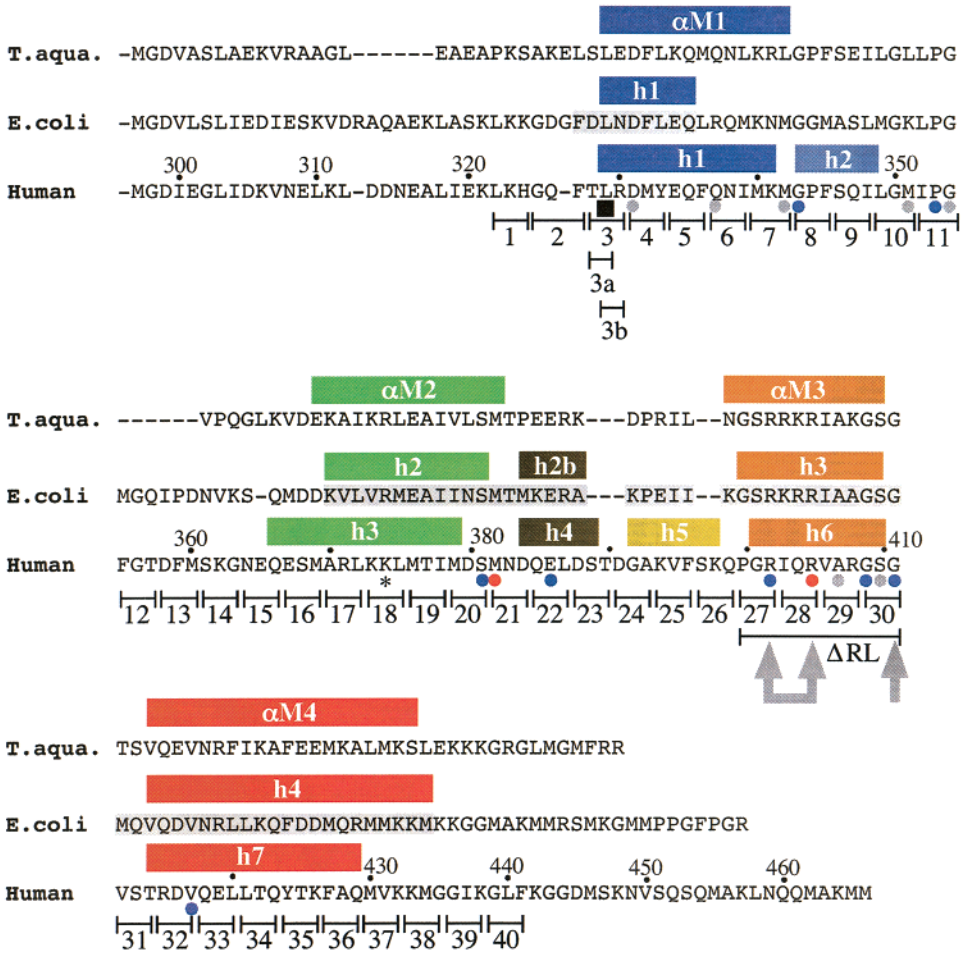

FIGURE 2: SRP54M-domain sequence alignment and secondary structures of *T. aquaticus* Ffh (*18*), *E. coli*. Ffh (*10*) and human ΔC1 (*19*). α-helical regions as determined by X-ray crystallography are shown above each sequence and named as in the original publications. Alignment gaps are indicated by dashes. The human sequence is numbered according to full-length SRP54 (*15*). Brackets mark the three amino acid residues that were altered to Alanine residues for each of the 40 constructs, numbered 1−40. It should be noted that an additional residue change had occurred in mutants A19 and A37 (see Table 1). The locations of mutants proteins 3a and 3b and the deletion in mutant polypeptide ΔRL are shown. Red dots mark invariant residues M382 and R405; residues conserved to greater than 90% are marked with blue dots; gray dots indicate residues that are conserved in 80−90% of representative SRP54 sequences (*2*). A Leucine residue corresponding to position 329 of human SRP54 reported in this communication to be critical for binding to SRP RNA and changed to an Alanine in mutant protein 3c is marked by a black square. The star marks a silent K374R change that was present in the ΔC1 polypeptide but absent in wild-type human SRP54. The two regions of *E. coli* Ffh that were visible in the crystal structure of the *E. coli* SRP core (*10*) are shown on a gray background. The gray arrows mark three residues that correspond to lethal phenotypes when altered at the equivalent positions of *Schizosaccharomyces pombe* SRP54 (*25*).

nonpolar character of this residue and displayed a binding activity of about 40% (Table 1).

It was interesting to note that certain mutations which abolished binding to SRP RNA corresponded to lethal phenotypes in *Schizosaccharomyces pombe* SRP54 (*25*). Examples of this correlation were the *S. pombe* SRP54 R398A/R401A double mutation (equivalent to R402A/R405A in human SRP54) and the *S. pombe* SRP54 G407P change which corresponded to human G411A (indicated by gray arrows in Figure 2). These findings provided support for the idea that binding of *S. pombe* SRP54 occurred in a way similar to how SRP54 of higher eukarya bound to SRP RNA. Furthermore, the functional conservation of these residues indicated that the interaction between SRP54 and SRP RNA may be required for survival of archaea and higher eukarya.

Analysis of Complexes. Two similar but significantly different conformations of the SRP54M domain had been determined by X-ray crystallography. In the structure of the *Thermus aquaticus* Ffh trimer, a short wide groove was available to a hydrophobic loop (the "finger loop") from a neighboring molecule. Residues located within and flanking α-helix M3 (see Figure 2) were predicted to be in contact with RNA (*18*). The same overall conformation was present in the structure of the *E. coli* SRP core where the signal peptide binding groove was found to be empty (*10*). Interestingly, structure was assigned not only to the interface between 4.5S RNA and the Ffh protein but also to α-helix 1 of *E. coli* Ffh (shown on a gray background in Figure 2), whereas the structure of the connecting region remained undetermined. This shorter visible region contained a Leucine at position 331 as part of the hydrophobic core. In the structure of the h54m dimer (*19*), helices 1 and 2 extended from the RNA binding domain to form a long narrow groove which was occupied by a signal peptide mimic from a neighboring molecule. This interpretation was consistent with the known α-helical character and general design of signal peptides (*20*). Helices h3−h7 of human SRP54 and the

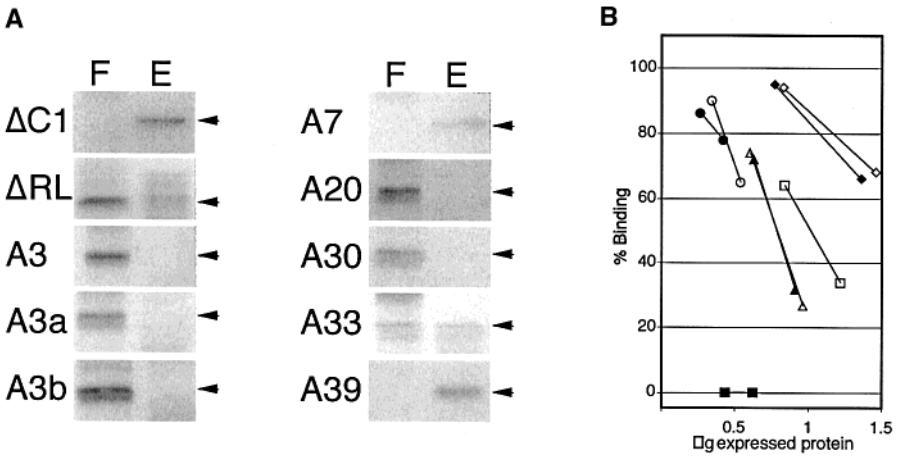

FIGURE 3: (A) SDS PAGE of mutant polypeptides in the flowthrough (F) and eluate (E) after separation of complexes from unbound protein on DEAE Sepharose. Representative results are shown for ΔC1, ΔRL (missing residues at positions 400−411 in the SRP RNA binding site), and mutants A3, A3a, A3b, A7, A20, A30, A33, and A39. Arrowheads point to the various mutant polypeptides. The ΔRL deletion polypeptide was completely inactive but comigrated with *E. coli*-derived polypeptides. (B) Dependency of RNA binding activity on the amounts of expressed protein for h54m (open rhombus), mutant A7 (filled rhombus), A23 (open circles), A19 (closed circles), ΔC1 (open triangles), A29 (closed triangles), A26 (open squares), and mutant A3b (closed squares).

Table 1: RNA Binding Activities of SRP54-ΔC1 Mutants[a]

name	amino acid changes	ACT (%)	name	amino acid changes	ACT (%)
54M-ΔC1	none	100	A18	373-KKL-375 to AAA	100
ΔC1-ΔRL	12 residues deleted (P-400 to G-411)	0	A19	376-MTI-378 to AAA, R-371 to K†	100
			A20	379-MDS-381 to AAA	0
A1	322-LKH-324 to AAA	100	A21	382-MND-384 to AAA	0
A2	325-GQF-327 to AAA	100	A22	385-QEL-387 to AAA	0
A3	328-TLR-330 to AAA	0	A23	388-DST-390 to AAA	100
A3a	328-TL-329 to AA	5.8 ± 2.8	A24	391-DG-392 to AA	100
A3b	329-LR-330 to AA	0	A25	394-KVF-396 to AAA	0
A3c	329-L-329 to A	41.5 ± 9.6	A26	397-SKQ-399 to AAA	100
A4	331-DMY-333 to AAA	100	A27	400-PGR-402 to AAA	0
A5	334-EQF-336 to AAA	100	A28	403-IQR-405 to AAA	0
A6	337-QNI-339 to AAA	100	A29	V-406 to A, R-408 to A	100
A7	340-MKM-342 to AAA	100	A30	409-GSG-411 to AAA	0
A8	343-GPF-345 to AAA	100	A31	412-VST-414 to AAA	100
A9	346-SQI-348 to AAA	100	A32	415-RDV-417 to AAA	100
A10	349-LGM-351 to AAA	100	A33	418-QEL-420 to AAA	51 ± 17*
A11	352-IPG-354 to AAA	100	A34	421-LTQ-423 to AAA	33 ± 21*
A12	355-FGT-357 to AAA	100	A35	424-YTK-426 to AAA	100
A13	358-DFM-360 to AAA	100	A36	F-427 to A, Q-429 to A	100
A14	361-SKG-363 to AAA	100	A37	430-MVK-432 to AAA, G-436 to C†	100
A15	364-NEQ-366 to AAA	100	A38	433-KMG-435 to AAA	100
A16	367-ESM-369 to AAA	100	A39	436-GIK-438 to AAA	100
A17	371-RL-372 to AA	100	A40	439-GLF-441 to AAA	100

[a] The names of the various polypeptides, the introduced alterations, and the corresponding RNA binding activities (ACT) are shown. Results obtained with mutants A33 and A34 (labeled by *) were derived from four independent lysate preparations. Mutants A19 and A37 contained a fourth amino acid residue change (marked by †).

homologous bacterial regions formed similarly shaped RNA binding surfaces. However, in h54m, L329 was further away from the RNA binding site than in the bacterial homologues (Figure 4A).

Although a single SRP54 molecule is present in the assembled SRP (*4*), we detected dimers of human SRP54m (h54m) in solution, demonstrating that the dimeric state was not crystallographically induced. Thus, we considered the possibility that ΔC1 or h54m generated two RNA binding sites where each site was formed from residues of two penetrating molecules, as had been observed previously in the crystal structure (*19*). Another possibility for forming a functional RNA binding surface was a change in the conformation of a single molecule which would bring L329 closer to the RNA binding region (Figure 4B). To investigate these two conflicting scenarios, we determined the oligomeric state of ΔC1 and h54m in the absence and presence of SRP RNA by using gel filtration and sucrose gradient centrifugation.

Figure 5A shows the gel exclusion profiles for ΔC1 and h54m carried out at 4 °C. In the absence of RNA, two predominant peaks were observed. About 72% of ΔC1 was recovered as a slower-moving population of molecules (labeled "M") with a determined molecular weight of 19 317 ± 580 Da, consistent with the theoretical molecular weight (19 105 Da) of a monomer. The molecular weight of the faster moving peak (labeled "D") was 33 517 Da, in agreement with the mobility of a ΔC1 dimer in which the

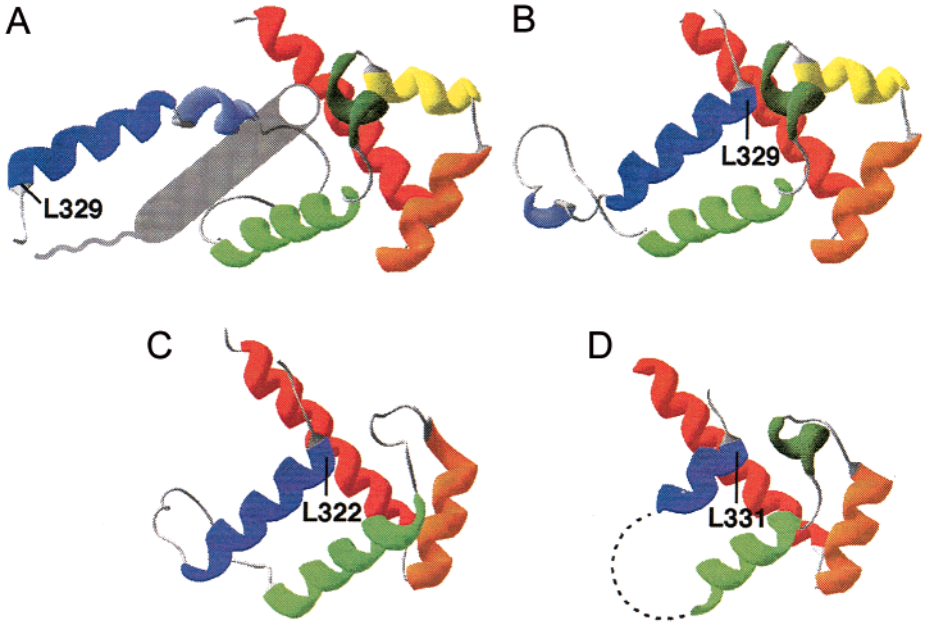

FIGURE 4: Homologous M-domain structures. (A) h54m as present in the crystal structure of the dimer (*19*) showing one molecule in color and the signal peptide mimic from the second molecule as a gray cartoon. The large white dot indicates the N-terminus of the signal peptide. (B) Hypothetical alternative conformation of the h54m monomer in which L329 is closer to the RNA binding site. (C) *T. aquaticus* Ffh M-domain as seen in the crystal structure of the Ffh trimer (*18*). (D) *E. coli* Ffh in the complex with 4.5S RNA (*10*). Helices are color-coded as in Figure 2, and the Leucine residues that correspond to L329 in human SRP54 are numbered.

two molecules had formed a single elongated unit (*19*). When we analyzed h54m, 63% was in the dimeric form (25 845 ± 1567 Da), whereas the slower moving population migrated at 14 594 ± 406 Da as a monomer (predicted to be 13 581 Da).

Complexes of ΔC1 and h54m with *M. jannaschii* SRP RNA (labeled "C", in Figure 5A) migrated only slightly faster than the free RNA, indicating that a single protein molecule had reacted with one RNA chain. The decreased monomer/dimer ratio of free ΔC1 also suggested the binding of a monomer. When SRP RNA was added to h54m, the monomer/dimer ratio increased, and there was also a slight increase in the amount of the monomer (see insert in Figure 5A, right panel), suggesting that the RNA was able to shift the monomer/dimer equilibrium toward the monomeric state. Complexes were formed effectively in experiments carried out at room temperature when only monomers were present (not shown). These result illustrated the potential of SRP RNA to shift the equilibrium away from the h54m dimer and form heterodimeric ribonucleoprotein particles.

Both the h54m monomer and the dimer could be used as starting materials for crystallization of the dimeric form, implying a conversion between the two states in the absence of SRP RNA (Clemons, personal communication). Although the crystals of the h54m dimer remained stable at room temperature, it is interesting to note that ΔC1 and h54m existed only as monomers when analyzed by gel filtration at room temperature (not shown).

Sucrose gradient centrifugation was used to examine complexes between the *M. jannaschii* Δ35 RNA (*24*) and proteins ΔC1 and 54m, as described in Materials and Methods. The addition of the RNA indicated that the vast majority of the polypeptide within the preparations was capable to bind to the RNA. Figure 5B shows that the complexes migrated between the mobilities of free Δ35 RNA (44 558 Da) and full-length *M. jannaschii* SRP RNA (106 816 Da) labeled "c" and "b", respectively. Due to the broad distribution of the sample within the gradient, we could not exclude the possibility that oligomers of higher order were present as well. However, substantial amounts of large multimeric complexes that would have formed if two RNA molecules had interacted with the hypothetical dimeric forms of ΔC1 or 54m were not detected.

Model of the h54m RNA Complex. Our systematic site-directed mutagenesis of the M-domain of human protein SRP54 combined with studies of the monomer/dimer ratio of the ΔC1 or h54m polypeptides in solution (described above) demonstrated that a single polypeptide and not the dimeric form bound to SRP RNA. This finding was consistent with the presence of a single SRP54 molecule in the assembled SRP but could only occur if the small region that included Leucine at position 329 of SRP54 became part of the hydrophobic core as a consequence of a conformational change in the signal peptide binding groove.

For the interpretation of the results in three dimensions, we constructed a model for the RNA-bound form of the relevant portions of the human SRP54 protein from the coordinates of the h54m dimer (PDB accession 1QB2) by combining residues 326−344 from chain A with residues 345−434 of chain B (*19*). This manipulation required a reorientation of the large loop between helices 2 and 3. A continuous structure was obtained by a rotation around K362, followed by bond adjustments at residues F-345 and K-362. The crystallographically well-defined loop conformation and the F359/F355-stack (*19*) remained undisturbed. The phylogenetically conserved structures of human and *M. jannaschii* helix 8 and were built using the RNA modeling program ERNA-3D as described in Materials and Methods. The relevant RNA and protein segments were superposed onto the structure of the *E. coli* SRP core (*10*) and aligned

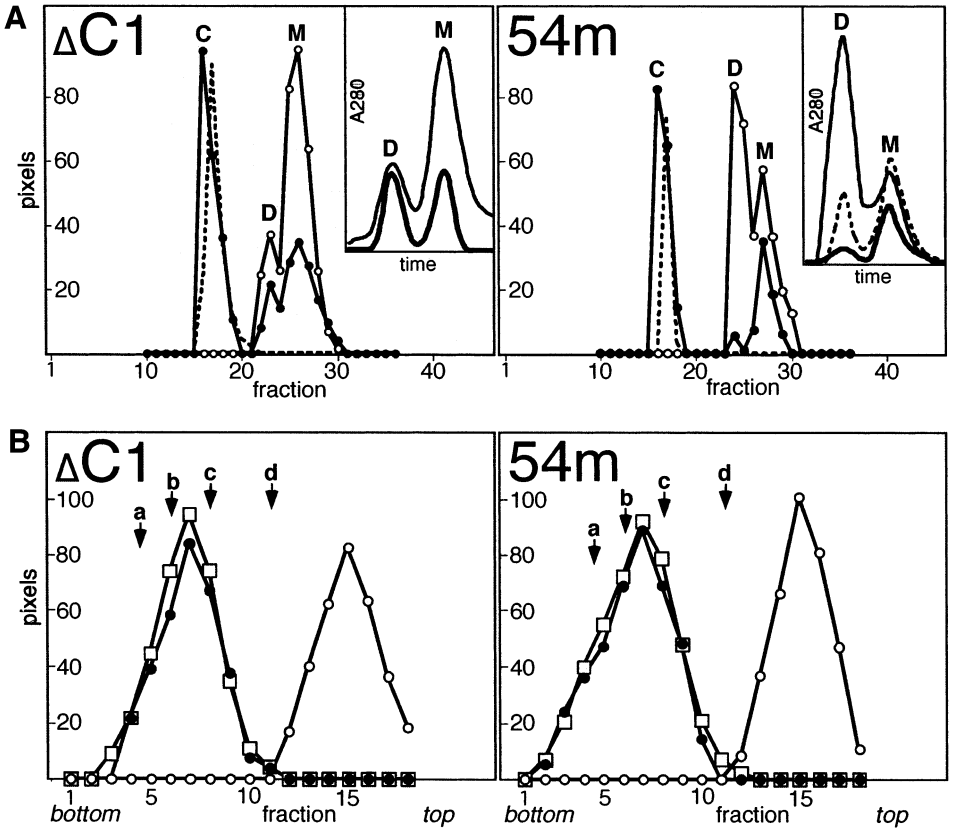

FIGURE 5: Analysis of ΔC1 and h54m complexes. (A) Separation of ΔC1 (left panel) or 54m (right panel) by gel filtration on Superdex 75 at 4 °C. Fraction aliquots were analyzed by SDS PAGE (for protein) and electrophoresis on 2% agarose gels (for RNA). The number of pixels in the bands of the digitized photos were determined using NIH Image software (*29*). Open circles mark the profiles of the free proteins; closed circles are for profiles that were obtained when *M. jannaschii* SRP RNA was added to the binding reaction as described in Material and Methods. The dashed lines indicate the mobility of free *M. jannaschii* SRP RNA. In each panel, the insert shows the A_{280} trace in the mobility range of the free proteins without (thin lines) or with added SRP RNA (thick lines, and also the dashed line in the 54m panel insert). The monomer (M), dimer (D), and the complex (C) peaks are labeled. (B) Sucrose gradient centrifugation analysis of proteins ΔC1 or h54m (6−10 μg) free or in complex with 15−30 μg of *M. jannaschii* Δ35 SRP RNA (*24*). The top and bottom of the gradients are labeled as such. Unbound proteins are represented by lines with open circles. Fractions were analyzed by SDS PAGE and agarose gel electrophoresis. Filled circles indicate complexed protein and open squares represent complexed Δ35 SRP RNA. The migration distances of four marker RNAs are shown by arrows labeled **a** ("monster" SRP RNA, 148 788 Da, (*11, 30*)), **b** (*M. jannaschii* SRP RNA 106 876 Da), **c** (*M. jannaschii* Δ35 RNA 44 558 Da), and **d** (tRNA, 24 646 Da).

in 3-D using conserved amino acid residues (see Figure 2) as landmarks.

Figure 6 shows the molecular model of the human ribonucleoprotein complex, including the region of SRP54 that had been targeted by systematic site-directed mutagenesis. Mutations that abolished the RNA binding activity were in close proximity to the RNA, whereas residues that reduced RNA binding or yielded active polypeptides were predominant within the signal peptide binding region (Figure 6A,C). Examples of residues within 3 Å of the RNA that, when altered, abolished binding completely were D379 and S381 (mutant protein A20), M382 and N383 (A21), Q385 (A22), R402 (A27), R405 (A28), and G409 and S410 (mutant protein A30). An exception was T377 of mutant protein A19, which yielded an active polypeptide. However, this residue was located near the edge of the RNA protein interface and evidently not required. Mutant protein 29 was active although V406 and R408 were within 5 and 4 Å of the RNA. We noted, however, that a wild-type Alanine was present at position 407 and that the *E. coli* Ffh sequence contained an Alanine residue at the position corresponding to R408 (see Figure 2). Both facts suggested that changes of these two residues did not disrupt RNA binding or that the Alanines contributed to the formation of a more stable complex. L420 and L421, altered in mutant polypeptides A33 and A34, were not in direct contact with RNA but appeared to link helices 3 and 7, which explained their intermediate activities. In the inactive mutant protein A25, F396 was only 6.6 Å away from the bulged Adenosine at position 183 of SRP RNA and separated by 4.5 Å from the L329 residue believed to be part of the hydrophobic core and implicated indirectly in the binding to SRP RNA. Another reason for the lost activity of mutant A25 might have been a destabilization of an the interaction between helices 4 and 5 by the V395A change.

Role of SRP RNA in Signal Peptide Recognition. Analysis of the oligomeric states of ΔC1 and h54m demonstrated the ability of these polypeptides to form dimers in solution. In the crystal structure of the h54m dimer, each molecule mimicked the interaction of SRP54M with a signal peptide bound to a long narrow groove (*19*). The addition of SRP RNA shifted the equilibrium to the monomer and lead to the formation of a simple complex containing a single polypeptide chain bound to one RNA molecule. When combined with data obtained by systematic-site directed mutagenesis, these results suggested that a change in the shape of the signal peptide binding groove was required in

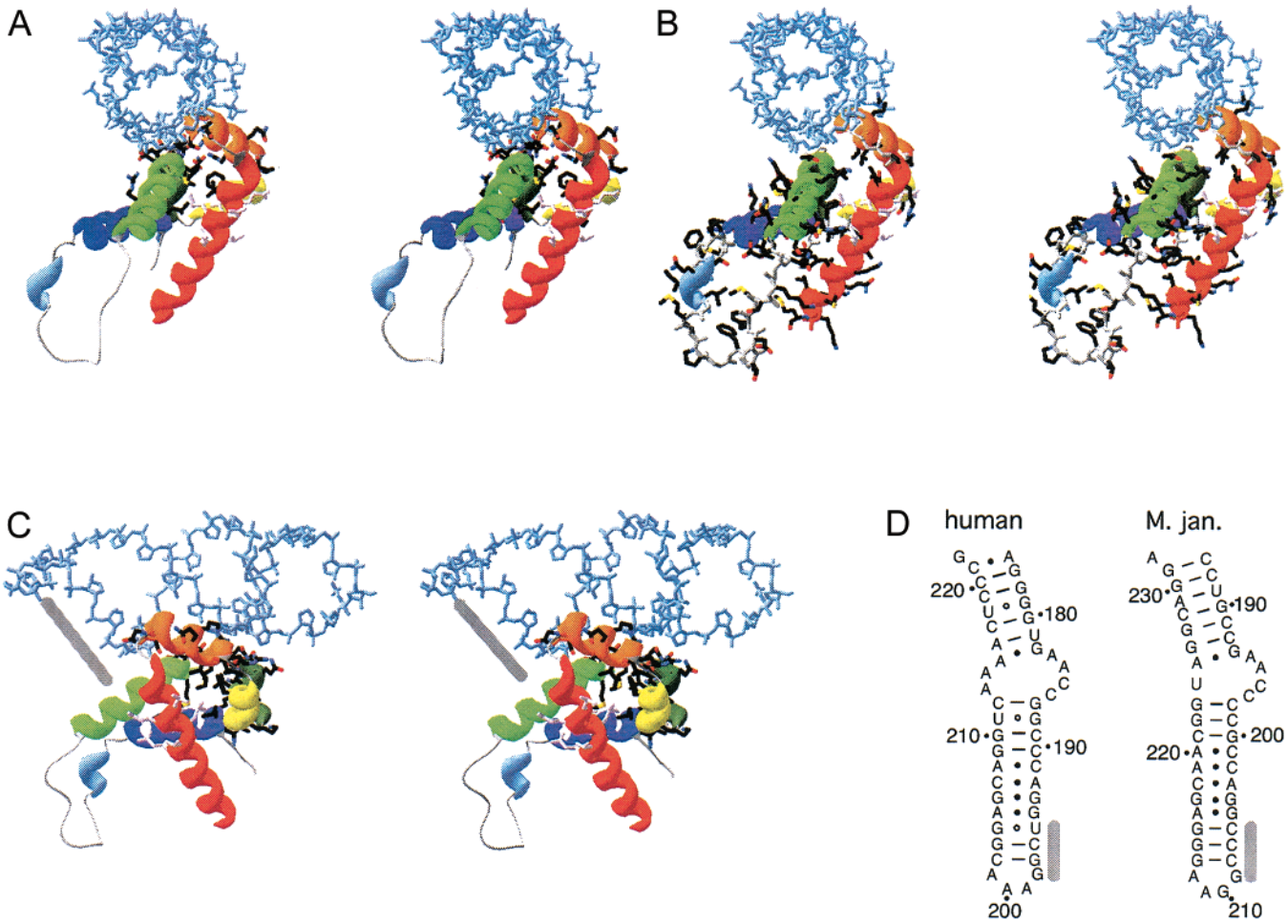

FIGURE 6: (A−C) Stereoviews of the complex of human SRP54m (h54m) with SRP RNA helix 8 derived by homology modeling using the crystal structure of the h54m dimer (*19*) and the *E. coli* Ffh core (*10*). In panels A and C, the carbon bonds of side-chains of h54m which abolish binding to SRP RNA (see Table 1) are drawn in black. Panel B shows the side-chains of mutants which did not affect SRP RNA binding. Residues changed in mutants A33 and A34 that showed intermediate RNA-binding activities are shown in pink. Helices are color-coded as in Figures 2 and 5. Panel D shows the secondary structure diagrams of human, and *Methanococcus jannaschii* (M. jan.) SRP RNA helix 8 with Watson−Crick base pairs represented by lines, G−U interactions by open circles, and noncanonical interactions by dots. Numbering is in increments of 10 according to the full-length molecules. The gray bars in panels C and D mark the phosphate ridge that may be in contact with the signal peptide.

order to bring L329 in closer proximity to the RNA. The distance between L329 and the RNA was 9.7 Å in the model of the h54m monomer with SRP RNA helix 8 (Figure 6). Similarly, the distance between the homologous L331 of *E. coli* Ffh and 4.5S RNA (*10*) was 11.4 Å. In both structures, the important Leucine residue was unable to interact with helix 8 directly but was located within the hydrophobic core surrounded by residues that in turn were in more intimate contact with the RNA.

Across species, position 329 of human SRP54 is conserved as a nonpolar bulky residue. Leucine is present in 76% of representative SRP54 sequences (*2*), but Phenylalanine (12%), Tyrosine (5%), Valine (3%), Isoleucine (2%), and Methionine (2%) occur in the SRP54 proteins of other organisms. Consistent with the phylogenetic data, a mutant protein with a single residue change from Leucine 329 to an Alanine (another hydrophobic but less bulky amino acid residue) displayed an SRP RNA binding activity of 41.5% (Table 1). Although this result indicated that a bulky residue was preferred at position 329, a significant binding activity was retained, and thus a contribution by the two neighboring amino acid residues could not be excluded.

An intriguing possibility for the signal peptide to bind to the SRP RNA was proposed first by Batey et al. in 2000 (*10*). The positive charges at the N-terminus of the emerging signal peptide were suggested to interact with a negatively charged phosphate ridge of the 4.5S RNA. Because the topologies of the *E. coli* 4.5S/Ffh complex and the model of the human complex were similar, there was the potential that the signal peptide interacted with SRP RNA also in the human system. Candidates for this interaction were the phosphates of residues 195−198 in the distal portion of helix 8 (marked by gray bars in Figure 6, panels C and D).

During SRP-mediated protein targeting, SRP54 may be transiently removed from the RNA to adopt the extended conformation represented by the structure of the h54m-dimer (*19*) and thus be capable of interacting intimately with the emerging signal peptide. A change of the shape of the signal peptide binding groove from a long narrow to a short wide conformation may occur when the protein is approached by the SRP RNA. This transformation would bring the small region centered around a bulky nonpolar amino acid (L329 in the case of human SRP54) in closer proximity to the RNA. In the RNA-bound conformation, SRP54 would bind to the

signal peptide more loosely within a short wide groove, as seen in the "finger loop" structure of the *T. aquaticus* Ffh trimer (*18*). This would allow the N-terminus to interact with a phosphate ridge in the distal portion of helix 8 and "pull out" from the groove. Finally, the signal peptide would be released to restore the free unbound state of the SRP. This proposed sequence of events implies a role for SRP RNA and a bulky nonpolar amino acid residue in the binding and release of signal peptides. It is currently unclear which state represents the membrane-bound form of the SRP and when, precisely, GTP hydrolysis occurs.

CONCLUSION

Our previous crystallographic study (*19*) indicated significant differences in the shape of the signal peptide binding groove between human SRP54 and the bacterial Ffh proteins. Here, we advocate that protein SRP54 changes its conformation in response to the signal peptide and the SRP RNA as part of a mechanism of SRP-mediated signal peptide binding and release used by all organisms. Although we can only speculate that a long narrow groove forms also in the bacterial Ffh, the conserved features of the RNA−protein interface suggest that the potential to change the shape of the signal peptide binding pocket has been preserved as well. A small region, including a bulky nonpolar residue in the M-domain of human SRP54, was important for promoting binding and may be used to communicate the conformation change to the RNA. In the model of the h54m helix 8-complex, this residue is only 4.5 Å away from a Phenylalanine at position 396. In turn, F396 is close to the two Adenosine residues at positions 183 and 184, which form the asymmetric bulged loop in the proximal part of human SRP RNA helix 8 (Figure 6). Future experiments will be directed toward a more detailed understanding of the structures of each proposed state including the postulated signal peptide−RNA interaction. Also, it will be necessary to address the role of the G-domain of SRP54 and determine the step at which GTP hydrolysis occurs. Finally, although technically difficult, it will be important to study complexes that contain true signal peptides.

MATERIALS AND METHODS

Mutants of Protein ΔC1. Plasmid SRP54-ΔC1 (*21*) was used as template in PCR site-directed mutagenesis reactions with a single mutagenic primer (*27*). Compared to human SRP54, the ΔC1 polypeptide contained an inconsequential Lysine to Arginine change at position 364. Amplifications using *Taq* DNA polymerase were carried out in a Rapid-Cycler (Idaho Technology, Inc.) for 35 cycles using steps of 94, 45, and 72 °C at each cycle. Oligonucleotides 5′-GCTCAGCTGGTCCTGCCTGCGAAATTAATACGACTCACT-3′ and 40 different mutagenic oligonucleotides were used in the reactions. The mutagenic oligonucleotides had at their center three Alanine codons and a *Not*I restriction site (GCGGCCGC) flanked on either side by nine to 14 residues. Oligonucleotide 5′-CTCTTGTTGATACTTGTTTACTAAAAAC-3′ was used in the construction of the nonbinding deletion mutant ΔRL. Amplified DNAs were purified by electrophoresis on 1% agarose gels followed by centrifugation through 3MM paper. A single-step extension was carried out using the first PCR product as primer and pSRP54-ΔC1 DNA as template in a Thermal Cycler (Perkin-Elmer Cetus) for 5 min at 95 °C, 2 min.at 37 °C, and 10 min at 72 °C. Oligonucleotides 5′-GCTCAGCTGGTCCTGCCTGC-3′ and 5′-GCTAGTTATTGCTCAGCGG-3′ designed to obtain the full-length ΔC1 derivative were then added and amplifications were carried out for 25−30 cycles with steps of 30 s at 95 °C, 2 min at 30−60 °C, and 2 min at 72 °C at each cycle. The PCR products were cleaved with *Nco*I and *Xho*I, purified by agarose gel electrophoresis, and ligated to *Nco*I and *Xho*I-digested pET23d (Novagen). Competent *E. coli* DH5-a cells were transformed and grown overnight at 37 °C on LB agar plates containing 200 μg/mL Ampicillin. DNAs from individual colonies were prepared and screened with *Not*I, *Nco*I, and *Xho*I. Mutant sequences were confirmed using Sequenase Version 2.0 (United States Biochemicals).

Synthesis of SRP RNAs. Human and *Methanococcus jannaschii* SRP RNAs were synthesized by runoff transcription with T7 RNA Polymerase using the MEGAshortscript kit (Ambion) and *Dra*I-digested plasmid DNAs of phR (*28*) and pMjSR (*24*). A 20 μL reaction contained 2 μg of DNA, 2 μL each of 75mM ATP, CTP, GTP and UTP, and 2 μL of enzyme mix. Samples were placed in a 37 °C incubator for 4 h, 2 units of DNaseI were added, and incubation was continued for 15 min. Reactions were terminated by addition of 115 μL of water and 15 μL of 5M ammonium acetate, 100 mM EDTA, pH 8.0. The RNA was recovered by adding 2 volumes of ethanol followed by a 15 min incubation at −20 °C and centrifugation at 4 °C. The pellet was washed with 500 μL of 80% ethanol, air-dried at room temperature, and dissolved in 50 μL of water. RNA concentrations were determined by co-electrophoresis of sample aliquots with known amounts of *E. coli* 5S ribosomal RNA, followed by ethidium bromide staining and quantitative analysis of the digital photographs using Quantity One (Bio-Rad) software.

Expression and binding activities of mutant polypeptides. Competent BL21(DE3) pLysS cells (Novagen) were transformed with the mutant plasmid DNAs and grown overnight on LB agar plates containing 200 μg/mL Ampicillin and 34 μg/mL Chloramphenicol. A small number of colonies were transferred to 2.5 mL LB containing Ampicillin and Chloramphenicol to achieve an A_{600} of approximately 0.1, followed by shaking at 37 °C for 1 h. Synthesis of mutant polypeptides was induced by addition of IPTG to 1mM and incubation for 2 h. Bacteria were harvested by centrifugation, washed once with 200 μL of 50mM Tris-HCl, 100mM NaCl, pH 8.0, and stored as pellets at −70 °C. Cell pellets were resuspended in 100−200 μL binding buffer (50 mM Tris-HCl, pH 7.9, 300 mM KOAc, 5 mM $MgCl_2$, 1 mM DTT, 50% glycerol), frozen at −70 °C for 15 min, and placed on ice for 15 min. Lysates was subjected to centrifugation for 15 min at 4 °C. The supernatant was used directly to determine RNA binding activities. Three cycles of freeze/thaw were carried out for mutant polypeptides A4, A15, A17, A20, A33, and A34 to recover more soluble protein. The lysates were stored at −20 °C.

SRP RNA binding activities were determined in a reaction volume of 100 μL of binding buffer, with 10 μg of *M. jannaschii* SRP RNA or 5 μg of human Δ35 SRP RNA and variable amounts of lysate followed by an incubation at 37 °C for 10 min. In reactions with human RNA, 2.8 μg of purified human protein SRP19 (*23*) was added and incubated,

followed by the addition of lysate and a second incubation at 37 °C for 10 min. Samples were loaded onto a 80 μL-bed volume DEAE-Sepharose Fastflow column prepared in an aerosol barrier tip (Continental Lab Products) and equilibrated in 50 mM Tris-HCl, pH 7.9, 300 mM KOAc, 5 mM $MgCl_2$, and 1 mM DTT. The flowthrough and 300 μL of 300 mM KOAc-buffer wash were combined (flowthrough, F), and RNA-bound protein was eluted with 400 μL of 1 M KOAc-buffer (eluate, E). Polypeptides were precipitated by the addition of 80 μL of TCA and incubation in an ice bath for 30 min. followed by centrifugation at 15 000 rpm for 20 min at 4 °C. The polypeptides in the pellets were dissolved in SDS loading buffer and analyzed by SDS PAGE on 15% gels and staining with Coomassie Blue R250. Protein quantities were determined from digitized photographs of the gels using NIH Image software (*29*) and a known amount of lysozyme to prepare a linear standard curve.

Protein purification. Proteins ΔC1 and h54m were purified using previously described procedures (*21*) with modifications. No ammonium sulfate fractionation (described below) was used in the preparation of ΔC1. In brief, *E. coli* BL21-(DE3) pLysS cells (Novagen) were transformed, and colonies were selected on LB plates containing 200 μg/mL Ampicillin and 34 μg/mL Chloramphenicol at 37 °C. Colonies were transferred to two 400 mL of liquid cultures at 37 °C, grown to an A_{600} of approximately 0.8, and transferred to 11.2 L LB with 200 μg/mL Ampicillin, 80 μg/mL Carbenicillin, and 34μg/mL Chloramphenicol medium in a 20 L fermenter vessel (Bioflow IV, New Brunswick Scientific). When the A_{600} reached approximately of 0.6, IPTG was added to 1 mM, and incubation was continued for 2 h. Cells were harvested by centrifugation, resuspended in lysis buffer (50mM sodium phosphate, 300mM NaCl, 5mM DTT, 1mM EDTA, pH 6.0), and stored at −70 °C. The approximate yield was 3 g of wet cells per liter. A 34 g sample of cells was lysed with 238 mL lysis buffer by incubation at 4 °C, followed by two centrifugation steps as described (*21*). The majority of ΔC1 and h54m were recovered in the supernatants. Samples were diluted 1:6 with 50mM sodium phosphate, 5mM DTT, and 1mM EDTA, pH 6.0, and loaded onto a Biorex 70 (Bio-Rad) cation exchange column (bed volume 138 mL). The column was washed with 50 mM sodium phosphate, 50 mM NaCl, 5 mM DTT, and 1 mM EDTA, pH 6.0, and the desired proteins were eluted with a linear gradient from 50 mM to 1 M NaCl. Protein from the pooled fractions was adjusted to pH 8.0 using 0.1M NaOH. $(NH4)_2SO_4$ was added at 4 °C to obtain 40% saturation, and after a incubation for 10 min on ice, the sample was subjected to centrifugation. The supernatant was collected and adjusted to 80% $(NH4)_2SO_4$. Again, the sample was incubated on ice and centrifuged, and the pellet was dissolved in 10mM sodium phosphate, 15 mM NaCl, 5 mM DTT, 1 mM EDTA, and 10% glycerol, pH 8.0. The protein was dialyzed against the same buffer, diluted 6-fold with phosphate buffer, and loaded onto a Q-Sepharose anion exchange column connected in series to a Heparin Sepharose column. The protein was eluted from the Heparin Sepharose column using a linear gradient from 15 mM to 1 M NaCl, and the pooled fractions were concentrated to 25 mg/mL using Centricon YM-10 devices (Amicon) and stored at −20 °C in 50 mM sodium phosphate, 250 mM NaCl, 5 mM DTT, 1 mM EDTA, 50% glycerol, pH 8.0. Typical yields were 1.5 mg of protein per g of wet cells. As analyzed by SDS PAGE, the purity of the proteins was approximately 90%.

Gel Filtration. Binding reactions were carried out in 50 mM Tris-HCl, 300 mM KOAc, 5 mM DTT, 1 mM $MgCl_2$, pH 7.9, containing between 50 and 150 μg of protein in a reaction volume of 100 μL. For the formation of complexes variable amounts (up to 350 μg/reaction) of *M. jannaschii* SRP RNA were added prior to a incubation for 10 min at 37 °C. Samples were loaded onto a Superdex 75 HR 10/30 column (Pharmacia) equilibrated in 50 mM Tris-HCl, 150 mM NaCl, 1 mM DTT, pH 6.5, at 4 °C at a flow rate of 0.4 mL/min. and. Migration was monitored by absorption at 280 nm. Mobilities were measured using a standard curve obtained from the migration distances of Thyroglobulin (670 000 Da), Gamma Globulin (158 000 Da), BSA (67 000 Da), Ovalbumin (44 000 Da), Myoglobin (17 000 Da), and Vitamin B-12 (1350 Da). Aliquots of the fractioned samples were analyzed by SDS PAGE and Coomassie Blue R250 staining (for proteins) or by electrophoresis on 2% agarose gels and ethidium bromide staining (for RNA). Protein and RNA amounts were determined by the analysis of digital photographs using NIH Image (*29*).

Sucrose Gradient Centrifugation. Reactions were prepared as for gel filtration but without glycerol in a volume of 400 μL. Protein amounts were between 6 and 10 μg, and *M. jannaschii* Δ35 SRP RNA (*24*) amounts were between 15 and 30 μg per reaction. Samples were incubated at 37 °C for 10 min and then loaded on top of a 10% to 40% sucrose gradient prepared in a 16 × 76 mm Quick-Seal tube (Beckman). Centrifugation was at 4 °C for 4.5 h at 55 000 rpm in a Beckman NVT65 rotor without brake applied. Gradient fractions were harvested from the bottom of the tube, and sample aliquots were analyzed by SDS PAGE and electrophoresis on 2% agarose gels as described above. In vitro transcribed "monster" SRP RNA (*11*, *30*) (148 788 Da), *M. jannaschii* SRP RNA (106 816 Da), *M. jannaschii* Δ35 RNA (44 558 Da), and tRNA (∼24 646 Da) were used as molecular weight standards.

Comparative 3-D Modeling of Complexes between SRP54m and Human SRP RNA. The coordinates of the h54m dimer ((*19*), PDB accession 1QB2) were exploited to model the h54m monomer by using the program ERNA-3D (*31*) on a Silicon Graphics Octane workstation. The homology modeling capabilities of the program were used to generate human SRP RNA helix 8 and the three-dimensional model of the human complex by superposing in 3-D the crystal structure of the *E. coli* SRP core (*10*). VCMD software (*32*) were used for refinement. The model is available from the SRP database at the URL http://psyche.uthct.edu/dbs/SRPDB/SRPDB.html.

ACKNOWLEDGMENT

We thank Anusuyadevi Mudalagiraiah for excellent technical assistance and Ching-Hui Yang for critical reading of the manuscript. This work was supported by NIH Grant GM-49034 to C.Z.

REFERENCES

1. Keenan, R. J., Freymann, D. M., Stroud, R. M., and Walter, P. (2001) The Signal Recognition Particle, *Annu. Rev. Biochem. 70*, 755−775.

2. Gorodkin, J., Knudsen, B., Zwieb, C., and Samuelsson, T. (2001) SRPDB (Signal recognition particle database), *Nucleic Acids Res. 29*, 169−170.
3. von Heijne, G. (1985) Signal sequences: the limits of variation, *J. Mol. Biol. 184*, 99−105.
4. Walter, P., and Blobel, G. (1983) Disassembly and reconstitution of the signal recognition particle, *Cell 34*, 525−533.
5. Römisch, K., Webb, J., Herz, J., Prehn, S., Frank, R., Vingron, M., and Dobberstein, B. (1989) Homology of 54K protein of signal-recognition particle, docking protein and two E. coli proteins with putative GTP-binding domains, *Nature 340*, 478−482.
6. Bernstein, H. D., Poritz, M. A., Strub, K., Hoben, P. J., Brenner, S., and Walter, P. (1989) Model for signal sequence recognition from amino-acid sequence of 54K subunit of signal recognition particle, *Nature 340*, 482−486.
7. Larsen, N., and Zwieb, C. (1991) SRP-RNA sequence alignment and secondary structure, *Nucleic Acids Res. 19*, 209−215.
8. Schmitz, U., Behrens, S., Freymann, D. M., Keenan, R. J., Lukavsky, P., Walter, P., and James, T. L. (1999) Structure of the phylogenetically most conserved domain of SRP RNA, *RNA 5*, 1419−1429.
9. Jovine, L., Hainzl, T., Oubridge, C., Scott, W. G., Li, J., Sixma, T. K., Wonacott, A., Skarzynski, T., and Nagai, K. (2000) Crystal structure of the ffh and EF-G binding sites in the conserved domain IV of Escherichia coli 4.5S RNA, *Structure Fold. Des. 8*, 527−540.
10. Batey, R. T., Rambo, R. P., Lucast, L., Rha, B., and Doudna, J. A. (2000) Crystal structure of the ribonucleoprotein core of the signal recognition particle, *Science 287*, 1232−1239.
11. Yin, J., Yang, C., and Zwieb, C. (2001) Assembly of human signal recognition particle (SRP): overlap of regions required for binding of protein SRP54 and assembly control, *RNA 7*, 1389−1396.
12. Rose, M. A., and Weeks, K. M. (2001) Visualizing induced fit in early assembly of the human signal recognition particle, *Nat. Struct. Biol. 8*, 515−520.
13. Diener, J. L., and Wilson, C. (2000) Role of SRP19 in assembly of the Archaeoglobus fulgidus signal recognition particle, *Biochemistry 39*, 12862−12874.
14. Romisch, K., Webb, J., Lingelbach, K., Gausepohl, H., and Dobberstein, B. (1990) The 54-kD protein of signal recognition particle contains a methionine-rich RNA binding domain, *J. Cell Biol. 111*, 1793−1802.
15. Gowda, K., Black, S. D., Moeller, I., Sakakibara, Y., Liu, M. C., and Zwieb, C. (1998) Protein SRP54 of human signal recognition particle: cloning, expression, and comparative analysis of functional sites, *Gene 207*, 197−207.
16. Gowda, K., Chittenden, K., and Zwieb, C. (1997) Binding site of the M-domain of human protein SRP54 determined by systematic site-directed mutagenesis of signal recognition particle RNA, *Nucleic Acids Res. 25*, 388−394.
17. Zopf, D., Bernstein, H. D., Johnson, A. E., and Walter, P. (1990) The methionine-rich domain of the 54 kd protein subunit of the signal recognition particle contains an RNA binding site and can be crosslinked to a signal sequence, *EMBO J. 9*, 4511−4517.
18. Keenan, R. J., Freymann, D. M., Walter, P., and Stroud, R. M. (1998) Crystal structure of the signal sequence binding subunit of the signal recognition particle, *Cell 94*, 181−191.
19. Clemons, W. M., Gowda, K., Black, S. D., Zwieb, C., and Ramakrishnan, V. (1999) Crystal structure of the conserved subdomain of human protein SRP54M at 2.1 A resolution: evidence for the mechanism of signal peptide binding, *J. Mol. Biol. 292*, 697−705.
20. Gierasch, L. M. (1989) Signal sequences, *Biochemistry 28*, 923−930.
21. Gowda, K., Clemons, W. M., Zwieb, C., and Black, S. D. (1999) Expression, purification, and crystallography of the conserved methionine-rich domain of human signal recognition particle 54 kDa protein, *Protein Sci. 8*, 1144−1151.
22. Chakrabartty, A., Kortemme, T., and Baldwin, R. L. (1994) Helix propensities of the amino acids measured in alanine-based peptides without helix-stabilizing side-chain interactions, *Protein Sci. 3*, 843−852.
23. Walker, P., Black, S., and Zwieb, C. (1995) Cooperative assembly of signal recognition particle RNA with protein SRP19, *Biochemistry 34*, 11989−11997.
24. Bhuiyan, S. H., Gowda, K., Hotokezaka, H., and Zwieb, C. (2000) Assembly of archaeal signal recognition particle from recombinant components, *Nucleic Acids Res. 28*, 1365−1373.
25. Althoff, S. M., Stevens, S. W., and Wise, J. A. (1994) The SRP54 GTPase is essential for protein export in the fission yeast Schizosaccharomyces pombe, *Mol. Cell. Biol. 14*, 7839−7854.
26. Gowda, K., and Zwieb, C. (1997) Determinants of a protein-induced RNA switch in the large domain of signal recognition particle identified by systematic site-directed mutagenesis, *Nucleic Acids Res. 25*, 2835−2840.
27. Nelson, R. M., and Long, G. L. (1989) A general method of site-specific mutagenesis using a modification of the Thermus aquaticus polymerase, *Anal. Biochem. 180*, 147−151.
28. Zwieb, C. (1991) Interaction of protein SRP19 with signal recognition particle RNA lacking individual RNA helices, *Nucleic Acids Res. 19*, 2955−2960.
29. Rasband, W. The NIH-Image program is available at http://rsb.info.nih.gov/nih-image/.
30. Yang, C., and Zwieb, C. (2001) Swapping of functional domains using a chimeric monster deletion mutagenesis strategy, *BioTechniques 31*, 724−728.
31. Müller, F., Doring, T., Erdemir, T., Greuer, B., Junke, N., Osswald, M., Rinke-Appel, J., Stade, K., Thamm, S., and Brimacombe, R. (1995) Getting closer to an understanding of the three-dimensional structure of ribosomal RNA, *Biochem. Cell Biol. 73*, 767−773.
32. Sommer, I., and Brimacombe, R. (2001) Methods for refining interactively established models of ribosomal RNA towards physico-chemically plausible structure, *J. Comput. Chem. 22*, 407−417.

BI025765T